AGU PUBLICATIONS

JGR

Journal of Geophysical Research: Atmospheres

RESEARCH ARTICLE
10.1002/2016JD025263

Key Points:
- Satellite observations of atmospheric CH_4 from GOSAT in the Amazon Basin are compared with aircraft profiles using stratospheric model data
- We show that GOSAT measurements agree with the extended aircraft profiles at three sites, while at two others GOSAT is up to 10 ppb higher
- Our results are encouraging evidence that GOSAT XCH_4 can help constrain models and provide new insights into tropical methane emissions

Correspondence to:
A. J. Webb,
ajw88@le.ac.uk

Citation:
Webb, A. J., et al. (2016), CH_4 concentrations over the Amazon from GOSAT consistent with in situ vertical profile data, *J. Geophys. Res. Atmos.*, *121*, 11,006–11,020, doi:10.1002/2016JD025263.

Received 22 APR 2016
Accepted 23 AUG 2016
Accepted article online 26 AUG 2016
Published online 17 SEP 2016

CH_4 concentrations over the Amazon from GOSAT consistent with in situ vertical profile data

Alex J. Webb[1], Hartmut Bösch[1,2], Robert J. Parker[1,2], Luciana V. Gatti[3,4], Emanuel Gloor[5], Paul I. Palmer[6,7], Luana S. Basso[3], Martyn P. Chipperfield[8,9], Caio S. C. Correia[3,4], Lucas G. Domingues[3,4], Liang Feng[6], Siegfried Gonzi[6], John B. Miller[10,11], Thorsten Warneke[12] and Christopher Wilson[5,8,9]

[1]Earth Observation Science Group, Department of Physics and Astronomy, University of Leicester, Leicester, UK, [2]National Centre for Earth Observation, University of Leicester, Leicester, UK, [3]Instituto de Pesquisas Energéticas e Nucleares–Comissao Nacional de Energia Nuclear–Atmospheric Chemistry Laboratory, Cidade Universitária, São José dos Campos, Brazil, [4]Greenhouse Gases Laboratory, Instituto Nacional de Pesquisas Espaciais, São Paulo, Brazil, [5]School of Geography, University of Leeds, Leeds, UK, [6]School of GeoSciences, University of Edinburgh, Edinburgh, UK, [7]NCEO, University of Edinburgh, Edinburgh, UK, [8]School of Earth and Environment, University of Leeds, Leeds, UK, [9]NCEO, University of Leeds, Leeds, UK, [10]Global Monitoring Division, Earth System Research Laboratory, National Oceanic and Atmospheric Administration, Boulder, Colorado, USA, [11]Cooperative Institute for Research in Environmental Sciences (CIRES), University of Colorado Boulder, Boulder, Colorado, USA, [12]Institute of Environmental Physics, University of Bremen, Bremen, Germany

Abstract The Amazon Basin contains large wetland ecosystems which are important sources of methane (CH_4). Spaceborne observations of atmospheric CH_4 can provide constraints on emissions from these remote ecosystems, but lack of validation precludes robust estimates. We present the first validation of CH_4 columns in the Amazon from the Greenhouse gases Observing SATellite (GOSAT) using aircraft measurements of CH_4 over five sites across the Amazon Basin. These aircraft profiles, combined with stratospheric results from the TOMCAT chemical transport model, are vertically integrated allowing direct comparison to the GOSAT XCH_4 measurements (the column-averaged dry air mole fraction of CH_4). The measurements agree within uncertainties or show no significant difference at three of the aircraft sites, with differences ranging from −1.9 ppb to 6.6 ppb, while at two sites GOSAT XCH_4 is shown to be slightly higher than aircraft measurements, by 8.1 ppb and 9.7 ppb. The seasonality in XCH_4 seen by the aircraft profiles is also well captured (correlation coefficients from 0.61 to 0.90). GOSAT observes elevated concentrations in the northwest corner of South America in the dry season and enhanced concentrations elsewhere in the Amazon Basin in the wet season, with the strongest seasonal differences coinciding with regions in Bolivia known to contain large wetlands. Our results are encouraging evidence that these GOSAT CH_4 columns are generally in good agreement with in situ measurements, and understanding the magnitude of any remaining biases between the two will allow more confidence in the application of XCH_4 to constrain Amazonian CH_4 fluxes.

1. Introduction

Methane (CH_4) is the second most important anthropogenic greenhouse gas [*Ciais et al.*, 2013] in terms of its radiative forcing effect. It contributes toward the formation of surface ozone and directly influences water formation in the stratosphere. Atmospheric CH_4 mole fractions have increased by approximately 150% since the beginning of the industrial era [*Ciais et al.*, 2013] with uncertainties in emissions ranging from 10 to 100% [*Kirschke et al.*, 2013]. From the 1980s to 1992 concentrations rose by an average of about 12 ppb (parts per billion) per year, before slowing throughout the 1990s to near-zero average growth between 2000 and 2006 [*Dlugokencky et al.*, 1994, 2003]. In 2007 concentrations began to rise again by an average of approximately 6 ppb yr^{-1} [*Rigby et al.*, 2008; *Nisbet et al.*, 2014] and have recently increased by approximately 12 ppb in 2014 and 11 ppb in 2015 (NOAA). The reasons for these changes are poorly understood, and currently, there is a large difference between bottom-up and top-down estimates of CH_4 emissions [*Kirschke et al.*, 2013]. Consequently, it is of great importance to study and better quantify CH_4 fluxes.

Global methane emission is estimated to be 556 ± 56 Tg CH_4 yr^{-1}, with 202 ± 35 Tg CH_4 yr^{-1} originating from natural sources (approximately 36%) [*Ciais et al.*, 2013]. Bottom-up approaches estimate that wetlands account for 20–40% of the global source of which 50–60% of these wetland emissions originate from the tropics [*Bloom et al.*, 2012]. Previous work reported that tropical emissions between 2003 and 2009 amounted to 111.1 Tg CH_4 yr^{-1} (approximately 20% of the total), 15–33% of which were from Amazonian wetlands [*Bloom et al.*, 2012]. Recently, *Wilson et al.* [2015] analyzed in situ aircraft measurements and concluded that Amazonian emissions contributed between 5.5 and 7.5% of global CH_4 emissions between 2010 and 2011. Pyrogenic CH_4 sources are also important, originating as a result of the incomplete combustion of biomass from deforestation and wildfires, contributing approximately 4.3–8.1% of global emissions [*Kirschke et al.*, 2013].

Melton et al. [2013] compared 10 different wetland models of varying complexity and operational methods and found there to be extensive disagreement between them in their simulations of wetland areal extent and CH_4 emissions in both space and time. They further write that atmospheric CH_4 observation data sets are inadequate to evaluate typical model fluxes and that this severely restricts our ability to model global wetland CH_4 emissions. Satellites could help to fill this gap in atmospheric data with their frequent and global coverage, which is complimentary to the existing in situ CH_4 measurements. Currently, however, tropical South America shows the largest discrepancy between satellite top-down and bottom-up estimates of wetland emissions (17–48 Tg CH_4 yr^{-1} and 39–92 Tg CH_4 yr^{-1}, respectively) [*Kirschke et al.*, 2013]. Many previous studies, including *Parker et al.* [2015] and *Dils et al.* [2014], have shown that satellite total column CH_4 data from GOSAT (Greenhouse gases Observing SATellite) [*Kuze et al.*, 2009] are consistent with ground-based measurements over temperate regions with a small bias (4.8–6.2 ppb), but there have been no published attempts to validate satellite data in the Amazon to our knowledge. GOSAT has typically been validated using TCCON (Total Carbon Column Observing Network) stations [*Wunch et al.*, 2011] of which there is one at Manaus in the center of the Amazon which measured XCH_4 for a 3 month period at the end of 2014, but due to the short operational period, it is not used in this study. Validation of GOSAT in the Amazon is now especially important as more studies begin to assimilate this satellite data into atmospheric CH_4 models [*Fraser et al.*, 2013; *Alexe et al.*, 2015] and find that tropical South America and tropical Asia yield the largest differences between the GOSAT data and forward model output [*Fraser et al.*, 2014]. Validating these satellite measurements is therefore critical to understand if the differences between models and satellites can reflect new insights into tropical methane fluxes that can improve emission models.

We report the first comparison between column-averaged dry air mole fractions of methane (XCH_4) from GOSAT and estimates of total column CH_4 based on aircraft profiles which we extrapolate linearly to the tropopause from their maximum measurement altitude of 4.5 km or 7.5 km above sea level (asl) and extend through the stratosphere using a dedicated stratospheric model. The 4.5 km and 7.5 km altitude flights were performed in separate campaigns by aircraft with different flight ceilings. Section 2 of this paper concentrates on these aircraft measurements, while section 3 details the GOSAT data and investigates the features seen by GOSAT over the Amazon. Sections 4 and 5 describe the method used to compare aircraft point measurements with satellite column measurements and an error analysis for the method, while section 6 contains the results of this comparison. In section 7 we discuss what impact the model XCO_2, which is built into our GOSAT retrievals, has on our results, and finally, in section 8 we summarize the findings and discuss our conclusions.

2. Aircraft Data

As part of the NERC (Natural Environment Research Council)/Fundação de Amparo à Pesquisa do Estado de São Paulo Amazonian Carbon Observatory (ACO) Project, air samples from aircraft have been collected approximately once a month since January 2013 at two sites in the Amazon and analyzed for greenhouse gas concentrations including CH_4. Measurements were performed at the Instituto de Pesquisas Energéticas e Nucleares laboratory relative to the WMO X2004 scale using samples captured in 0.7 L flasks (pressurized to 2.7 atm) as the aircraft descends in a spiral between approximately 7–8 km and 300 m asl, typically taking 17 approximately equally spaced samples [*Gatti et al.*, 2014]. The samples were taken between 12:00 and 13:00 local time, making them comparable in time with measurements from the GOSAT satellite at approximately 13:00 local time, and were only performed in clear-sky conditions. The uncertainty in these measurements (as defined by repeated measurements of whole air from a high-pressure cylinder) is ±2 ppb for CH_4.

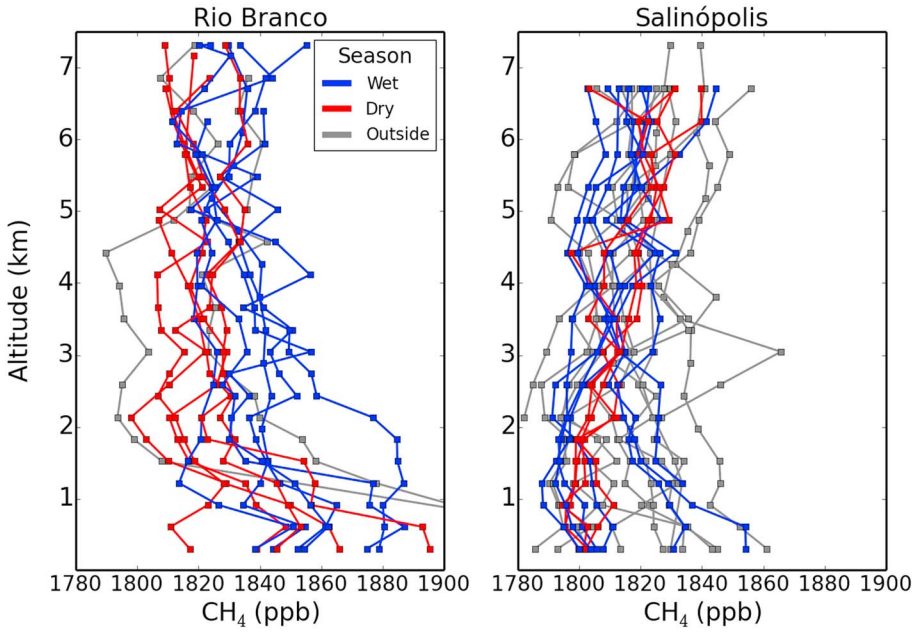

Figure 1. Amazonian Carbon Observatory aircraft measured CH_4 vertical concentration profiles taken between 2013 and June 2015 at Rio Branco and Salinópolis. Profiles measured between January–April are shown in blue, July–October in red, and May–June and November–December in gray.

Figure 1 shows every ACO aircraft profile up until the end of June 2015 color coded to represent the season in which they were measured (blue for the wet season, red for the dry season, and gray for intermediate months). The two sites (their location shown in Figure 2), located near Rio Branco (RBH) and Salinópolis (SAH), were chosen to best represent air before and after traveling across the Amazon Basin. This will be true most of the time since air entering the Amazon Basin is dominated by trade wind easterlies coming from the tropical Atlantic Ocean [*Miller et al.*, 2007]. To test this, we used the Met Office's Numerical Atmospheric-dispersion Modeling Environment (NAME) [*Jones et al.*, 2007] to run back trajectories where we simulate the release of 1 g of particles and calculate the locations of these particles 7 days before reaching either Rio Branco or Salinópolis at 7.5 km altitude. The data in Figure 2 show the seasonal average dosage normalized between 0 and 1 (of releases from every day in 2011) for both the wet and dry seasons and for both sites. This figure illustrates that over the year the majority of air to reach 7.5 km above Salinópolis originated (7 days earlier) from the east across the Atlantic Ocean, as was expected. For Rio Branco we see that the air has traveled from across the Amazon Basin from east to west. We use the same definition of the wet season as was used by *Gatti et al.* [2014] (approximately between January and April). *Gatti et al.* [2014] defined the dry season as the rest of the year, while we have excluded the two months between each season to account for yearly variations in the timing and length of the seasons, ensuring that our "dry season" measurements are not affected by the wet season overrunning or beginning earlier than usual (dry season in this study is represented by July–October). Figure 2 shows that in the wet season, as the Intertropical Convergence Zone moves farther south, the air originates from farther north than it does during the dry season.

The profiles in Figure 1 from the background site (SAH) typically have lower values of CH_4 throughout most of the altitude range than those at the inland site (RBH), especially for the first few levels above the surface (average CH_4 across all altitude levels and profiles is 1834 ppb for RBH and 1815 ppb for SAH). This difference in profile shape arises due to RBH being in the Amazon Basin where the surface air is likely influenced by local wetlands, while the coastal air measured at SAH will be relativity free from wetland influence. The wet and dry season profiles are more similar at SAH (1812 ppb and 1811 ppb, respectively), while there is a more distinct separation at RBH (1840 ppb for the wet season and 1825 ppb in the dry season), with the profiles measured in the wet season containing elevated CH_4 concentrations in the low and midaltitude range. We would expect to see enhanced CH_4 emissions in the wet season due to the increased flooded area from seasonal wetlands. The profiles show that during the wet season there is atmospheric uptake of CH_4 as the air travels from the

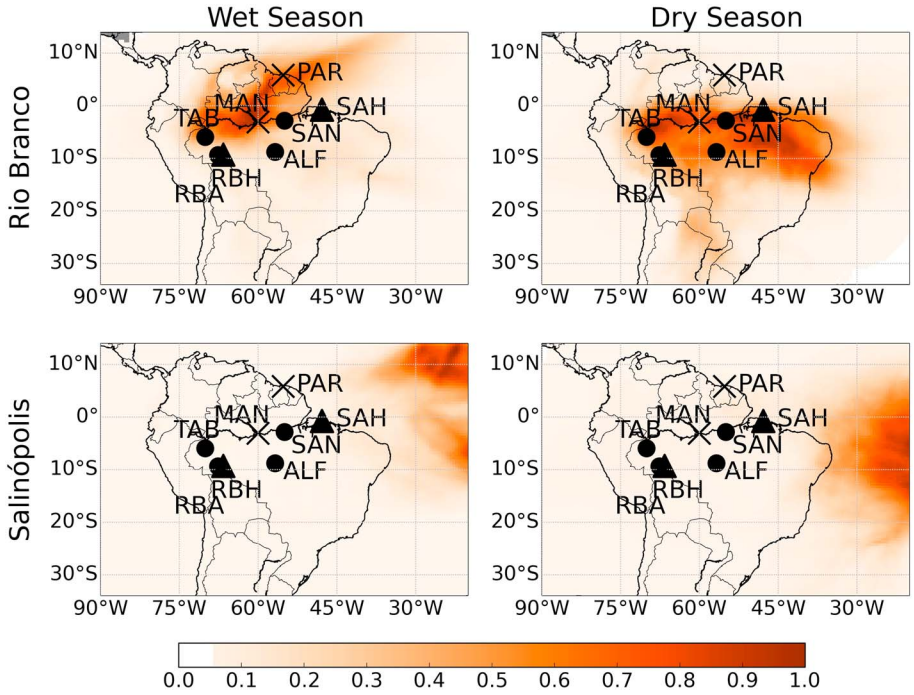

Figure 2. The mean location of incoming air sampled at (top row) Rio Branco and (bottom row) Salinópolis. This is the seasonal average location of air 7 days before reaching the site at 7.5 km altitude. An average over (left column) the wet season (January–April) and (right column) the dry season (July–October). The data shown are a normalized particle dosage in gsm^{-3} resulting from a 1 g release of particles at midday for every day in 2011, utilizing the NAME Numerical Atmospheric-dispersion Modeling Environment to calculate back trajectories based on meteorological data to track the particles back 7 days. The locations of the aircraft sites, RBA (Rio Branco AMAZONICA), RBH (Rio Branco ACO), SAH (Salinópolis), ALF (Alta Floresta), SAN (Santarém), TAB (Tabatinga) are shown in addition to the Paramaribo-FTS site (PAR) and Manaus TCCON site (MAN).

background site to the inland site at midaltitudes, while there is less of a difference near the surface and at higher altitudes.

In addition to the ACO profiles at the two sites, aircraft samples ranging from 300 m asl up to a height of 4.5 km from four sites across the Amazon Basin measured during the AMAZONICA project [*Gloor et al.*, 2012; *Wilson et al.*, 2015] are also used in this study. The sampling sites are at Rio Branco (RBA), Tabatinga (TAB), Alta Floresta (ALF), and Santarém (SAN) (shown in Figure 2). These measurements were performed using the same sampling and analysis techniques as the ACO flights, with approximately 12 samples over the altitude range. The flights operated at all four sites from 2010 and were typically performed twice monthly (where weather conditions allowed) until the end of 2012 at all sites and are still ongoing at Rio Branco.

3. GOSAT Observations Over the Amazon

GOSAT is the first dedicated satellite for the measurement of CO_2 and CH_4 columns [*Yokota et al.*, 2009]. It uses a Fourier transform spectrometer (FTS) to measure three channels in the shortwave infrared (0.758–0.775 μm, 1.56–1.72 μm, and 1.92–2.08 μm) and one in the thermal infrared region (5.5–14.3 μm). The satellite is in a Sun-synchronous orbit with an equator crossing time of approximately 13:00 local time and a repeat cycle of 3 days. Originally, the instrument was measured in a five-point across-track footprint, but from August 2010 this was changed to a three-point footprint where each location is measured three times; these locations are separated by approximately 150 km, each with a 10.5 km diameter field of view at the surface [*Kuze et al.*, 2009]. It occasionally enters target mode to view predetermined locations outside of the usual sampling pattern, and since 2014 a dithering observation mode has been used over the Amazon to increase the amount of clear-sky observations [*Kuze et al.*, 2016]. In our analysis we use only soundings where the retrieved surface pressure from the Oxygen A-band is less than 30 hPa different from that given by ECMWF (European Centre for Medium-Range Weather Forecasts); otherwise, they are flagged as cloud affected, leaving us with 79,562 cloud free soundings between 2009 and 2015 in or near the Amazon (between 10°N, 20°S, 85°W, and 30° W).

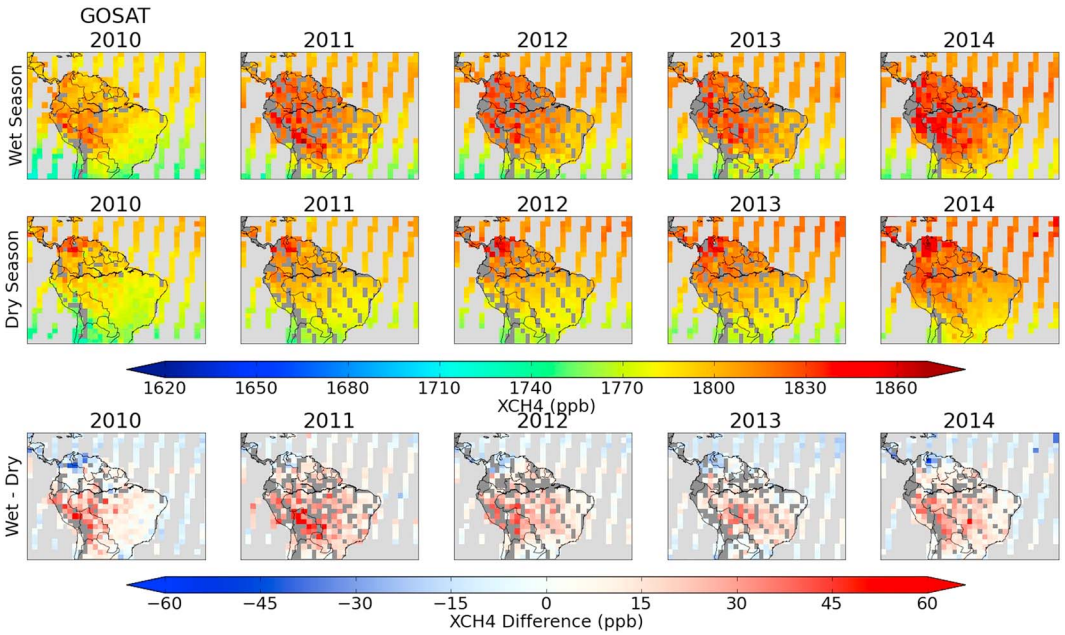

Figure 3. GOSAT XCH_4 averaged for the (first row) wet seasons (January–April) and (second row) dry seasons (July–October) in 2010 to 2014. (third row) The difference (wet season minus dry season) for the seasons in each year. The data are plotted to a 2° × 2° grid.

We use v161 of GOSAT L1B data from 2009 to 2014 which has been processed using v6 of the University of Leicester retrieval algorithm [*Parker et al.*, 2011, 2015] with CH_4 a priori from the MACC (Copernicus - Monitoring Atmospheric Composition and Climate) model v10-S1NOAA [*Bergamaschi et al.*, 2009]. The retrieval utilizes a CO_2 light-path proxy method similar to that employed by *Frankenberg et al.* [2006]. The algorithm retrieves XCO_2 and XCH_4 (the column-averaged dry air mole fractions of CO_2 and CH_4) to form the ratio of XCH_4/XCO_2 retrieved for two spectrally close windows, which is then multiplied by a modeled XCO_2. This procedure removes the majority of the effects of cloud and aerosol from the retrieval but does introduce a dependency on the error in the modeled XCO_2 [*Schepers et al.*, 2012; *Pandey et al.*, 2015, 2016]. To mitigate and quantify this uncertainty, we usually use a model ensemble as described in *Parker et al.* [2015]; however, as not all of the models of the employed ensemble are available for our entire time series of measurements we use only one XCO_2 model for consistency and validate this in section 7 of this paper. We use model fields from the University of Edinburgh (simulation version 2.02), which are based on the global chemistry transport model Goddard Earth Observing System (GEOS)-Chem v9.02. This is run at a spatial resolution of 4° × 5° and is driven by GEOS-5 meteorological analyses from the Global Modeling and Assimilation Office Global Circulation Model. The surface CO_2 fluxes are inferred from CO_2 mole fractions from NOAA's in situ Global Greenhouse Gas Reference Network, by using an Ensemble Kalman Filter [*Feng et al.*, 2009, 2011].

Figure 3 shows seasonally averaged GOSAT XCH_4 for the different wet and dry seasons between 2010 and 2014, including the difference between the seasons in each year. These maps show that northern South America (particularly around the border of Colombia and Venezuela) has higher concentrations in the dry season, while in the wet season the values are higher across the Amazon Basin farther south. These wet season enhancements are highest in the western Amazon, with the largest differences in or around Bolivia. *Hess et al.* [2015] studied the extent and location of wetland area in lowland Amazonia and show that there are extensive wetlands in Bolivia which are consistent with where we find the largest differences between the wet and dry seasons with GOSAT. The largest difference we observe is for 2011, which agrees well with observations that this was an anomalously wet year [*Gatti et al.*, 2014]. XCH_4 over the Atlantic Ocean shows little difference between the wet and dry seasons compared to those over land. This indicates that the enhanced concentrations in the Amazon for the wet season are a result of local emissions and not from XCH_4 transported across the Atlantic.

Ground-based XCH_4 measurements are also taken at Paramaribo, Suriname, which is north of the Amazon Basin (PAR in Figure 2), using a Bruker 120M Fourier transform spectrometer (FTS) [*Warneke et al.*, 2010]. Since

the launch of GOSAT in 2009 these measurements have been made during an approximately 2 week period in November each year. With data from five aircraft sites and from Paramaribo we can examine XCH_4 from GOSAT at multiple locations throughout the Amazon Basin.

4. Conversion of Aircraft Profiles to Total Column XCH_4

We convert aircraft profiles into total atmospheric columns following a method similar to that detailed by *Miyamoto et al.* [2013]. The method contains four steps: (1) extending the lowest aircraft measurement value down to the surface, (2) extrapolating between the aircraft profile and the tropopause, (3) estimating the stratosphere, and (4) conversion to a total column. First, the mole fraction between the lowermost aircraft measurement and the surface is assumed to hold the same values as the lowest aircraft measurement. This is reasonable for midday measurements because we expect there to be strong vertical mixing in the planetary boundary layer by 13:00 h. Second, the mole fraction throughout the altitude range between the uppermost aircraft measurement and the tropopause is assumed to be the same as at the highest aircraft measurement level since it is expected that at these higher altitudes the air will have become more well mixed. The tropopause altitude is calculated from ECMWF ERA-Interim data using the method outlined in *Reichler et al.* [2003], which uses a thermal definition of the tropopause based on a threshold lapse rate.

For the stratosphere we use a dedicated stratospheric model. This full chemistry simulation (run ID 570) of the TOMCAT atmospheric chemistry model from the University of Leeds was tailored for the stratosphere [*Chipperfield*, 1999]. This model run is constrained by observed global monthly mean surface CH_4 mole fractions and simulates atmospheric transport based on wind and transport fields from the ECMWF ERA-Interim reanalysis while also simulating the loss of CH_4 from chemical reactions. The model also uses the Prather second-order moments advection scheme to reduce numerical diffusion [*Prather*, 1986]. The run has a resolution of approximately 2.8° × 2.8° with 32 levels from the surface to 60 km and provides monthly mean output. From comparison against Atmospheric Chemistry Experiment (ACE)-FTS satellite profiles we find that the stratospheric CH_4 profile is well represented by TOMCAT. We calculated stratospheric XCH_4 for 163 ACE profiles within ±20° of the equator for 2008–2012 and compared these with TOMCAT XCH_4 which we calculated for the same altitude range. The mean difference in XCH_4 between ACE and TOMCAT was found to be 4.34% ± 4.58% (of the TOMCAT XCH_4). These differences are smaller than the expected uncertainty in the ACE profiles [*De Mazière et al.*, 2008].

Finally, the extended aircraft profile is converted into a total column by applying scene-specific pressure weighting functions and scene-dependent GOSAT averaging kernels to each level [*O'Dell et al.*, 2012]. We only use these cloud free GOSAT retrievals within a ±5° grid box around the aircraft location for the same day as the flight. Where there were no GOSAT observations on the same day the selection criteria were extended to an additional day on either side. The application of satellite averaging kernels results in the aircraft XCH_4 decreasing by 0.49–0.80 ppb, depending on the site. When there was no coincident GOSAT data, an average correction was applied, based on the corrections for other retrievals for the same site (0.49 ppb at RBA, 0.61 ppb at SAN, 0.51 ppb at TAB, 0.54 ppb at ALF, 0.57 ppb at RBH, and 0.80 ppb at SAH). Figure 4 shows an example profile before and after extension from an ACO flight on 16 August 2014. The average XCH_4 contribution of the aircraft data to the total column at the ACO sites RBH and SAH is 55.5% and 54.3%, respectively, while the AMAZONICA sites which only extend to 4.5 km contribute between 39 and 40% on average for the four sites. The part between the surface and the lowest aircraft measurement contributes approximately 0.5% to the total column. The extrapolated region between the top of the aircraft profile and the tropopause contributes approximately 50–51% for the AMAZONICA sites and 34–35% for the ACO sites. The stratospheric component composes approximately 10% of the total XCH_4.

5. Uncertainty Analysis

We estimated the uncertainty of the XCH_4 columns derived from the extended aircraft profile by assigning uncertainties to each section of the profile. Throughout the height of the aircraft profile the uncertainty used is from the air sample analysis. The uncertainty at the surface was assumed to be the same as the uncertainty in the lowest aircraft measurement. For the stratosphere, we use the method of *Wunch et al.* [2010]. This method shifts the stratospheric values up and down by 1 km to calculate the difference in total column, which is used as an estimate of the uncertainty in the location of the tropopause and therefore for the stratospheric contribution. Given the rapid decrease of CH_4 mole fraction in the stratosphere [*Wunch et al.*, 2010], the

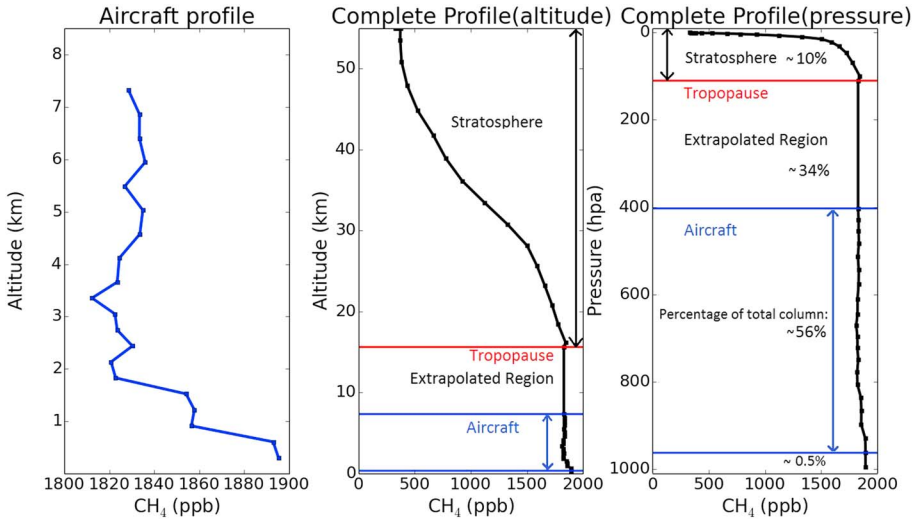

Figure 4. Example of the extended aircraft profile for the ACO flight at Rio Branco on 16 August 2014. (left) The measured aircraft profile. (middle and right) The final complete profile with altitude and pressure on the *y* axis, respectively. In Figure 4 (right), the percentage contribution to the XCH_4 from each part is displayed (these are average values for all of the RBH extended profiles).

tropopause height is a very sensitive parameter in constructing a total column using aircraft data. To address this, we compared our calculated tropopause altitudes with values from the NOAA National Centers for Environmental Prediction/National Center for Atmospheric Research Reanalysis 1 data set [*Kalney et al.*, 1996] for every flight and found average differences for each site of a few hundred meters, ranging from 359 ± 458 m to 763 ± 395 m (uncertainties are the 1 sigma standard deviations of the differences). These differences are small enough for the stratospheric shifting by ±1 km to suitably account for this uncertainty.

Between the maximum altitude of the aircraft measurements and tropopause the uncertainty was estimated by examining the variability of CH_4 in this vertical range from the ECMWF high-resolution MACC model for 2012 which is driven by ERA-Interim operational high-resolution meteorology, including real-time biomass burning. The horizontal resolution is 16 km with a 3-hourly output on 91 vertical levels. For each day in 2012 the XCH_4 partial column for this height range was calculated by taking the model value at either 4.5 km or 7.5 km to represent the highest aircraft measurement and using (a) the model concentrations for each level above these in this altitude range or (b) by using a constant value for these levels based on the concentration at this altitude. The difference in XCH_4 using these two methods then represents the estimated error of the method for this height range. The model output within ±5° of the site was used to calculate this error both daily and as a monthly mean. The median absolute deviation of all daily values of this error for a month gives an estimate of the variation in this altitude region and is used to describe the random uncertainties for this range. The median of the difference represents a systematic error with the method.

Figure 5 shows the results of the analysis for the monthly median and median absolute deviation for the extrapolated region of the aircraft profiles. We find the uncertainty for the extrapolated region for a flight height of 4.5 km to be between about 1.5 ppb and 4 ppb, with January and March for Rio Branco being exceptions with values up to 6 ppb. The median shows a relatively systematic behavior with a possible bias of between −4 ppb and +5 ppb which is dependent on the month. During the wet season the model data are typically higher for the extrapolated region than the linear method because there are higher CH_4 emissions and the model predicts enhanced features in the profile higher in the troposphere than it does during the dry season. The benefit of extending the height of the flights up to 7.5 km is shown by the difference in both the median standard deviation and the median in the extrapolated region between the two heights. The systematic uncertainty and the variability are decreased significantly when using higher altitude flights, suggesting that air higher in the troposphere is more well mixed. The average variability for Rio Branco decreases from 3.3 ppb to 2.1 ppb when going to the 7.5 km case, with the other sites behaving similarly (2.6–1.8 ppb for ALF, 2.9–1.6 ppb for SAN, and 3.0–1.8 ppb for TAB). The average absolute difference from zero across all months ranges from 2.1 ppb to 1.3 ppb when going to the 7.5 km case for Rio Branco, and again, results for the other sites are similar (2.7–1.1 ppb at ALF, 2.9–1.1 ppb for SAN, and 2.0–1.4 ppb for TAB).

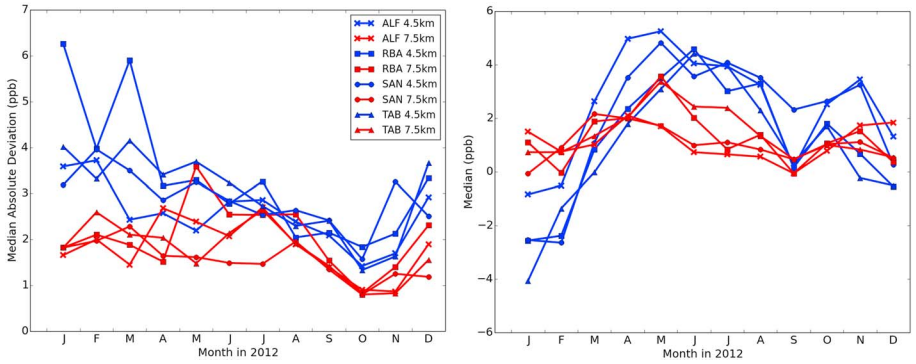

Figure 5. Estimated uncertainties for the region between the top of the measured profiles (4.5 km asl (blue) or 7.5 km asl (red)) and the tropopause, based on output from the MACC model. (left) The median absolute deviation (for each month of 2012) of the daily differences in XCH_4 between extrapolating linearly from 4.5 km or 7.5 km and taking the model levels of the high-resolution ECMWF model (the difference is model minus linear). (right) Showing the monthly median value of all the daily difference values as described in Figure 5 (left).

The combined random uncertainties (for all parts of the profile) in the aircraft total columns (mean across all flights = 3.6 ppb) are smaller than the individual GOSAT measurement uncertainties (mean single sounding precision across all flights = 10.8 ppb) and also than the standard error of the ensemble (reflecting the spread of GOSAT XCH_4 retrievals) of all coincident GOSAT data for a single day (mean for all days and flights = 6.6 ppb). In the majority of months the magnitude of the random error and systematic error combined is still smaller than the standard error of the coincident GOSAT soundings. Approximately 3–6% of the assigned random uncertainty in the total column is due to the actual aircraft measurements, about 42–52% is from the stratosphere, and the remaining 42–54% is from the extrapolated region. We also have estimated a systematic error from the extrapolated region of about 1.65 ppb and 1.13 ppb for the AMAZONICA and ACO sites, respectively; this is about 43% and 34% of the estimated random errors. For the remainder of this paper we use only the larger random error for the extended aircraft profiles.

6. GOSAT Comparison With In Situ Measurements

A time series of the XCH_4 inferred from the aircraft profiles and daily averaged GOSAT retrievals with a colocation criteria of ±5° is shown in Figure 6. For all sites, we find that XCH_4 calculated from the extended aircraft profiles shows a similar seasonal cycle to that seen from GOSAT methane data: enhanced methane in the wet season and lower values in the dry season. The figure shows a large variation in XCH_4 values of about 10–20 ppb for flights during the dry season in 2011 for Rio Branco and Alta Floresta and to a lesser extent around June–July 2010 for Rio Branco. Analysis of these differences at Rio Branco using the wind trajectory model Hybrid Single-Particle Lagrangian Integrated Trajectory [*Draxler and Hess*, 1997] suggests that they result from air traveling with different wind speeds. Generally, in the higher value cases air is slow moving and remains local to the site, whereas for lower values the wind speed is generally much higher, suggesting that the higher values result from slower moving air which has had more time to pick up local methane emissions. This is very promising as it indicates that GOSAT has the power to observe variations of XCH_4 over short time scales (between subsequent overpasses) and that it can see variations at regional scales within the Amazon Basin.

Figure 7 shows scatterplots between the aircraft profiles at each site and the daily average of the GOSAT data within ±5°. The corresponding correlations and biases for these comparisons are detailed in Table 1 for varying colocation criteria. We examine the correlation to understand the scatter and the variability between the aircraft and satellite measurements, while the offset indicates the bias between them. The average offset for each site is calculated with a linear fit between the data sets with the slope set to unity, as illustrated in Figure 7.

The offsets at Rio Branco are within their uncertainties for both the lower altitude AMAZONICA flights and the higher altitude ACO flights (−1.9 ± 2.2 ppb for RBA and 3.6 ± 4.3 ppb for RBH), with the larger uncertainties at RBH a result of having four times fewer flights. At the other sites GOSAT is on average higher by a few parts per billion than the aircraft values, and the bias is larger than the variability (3.6 ± 1.7 ppb for SAN, 8.1 ± 2.1 ppb for ALF, 6.6 ± 2.6 ppb for TAB, and 9.7 ± 2.8 ppb for SAH). A student's *t* test calculated on these

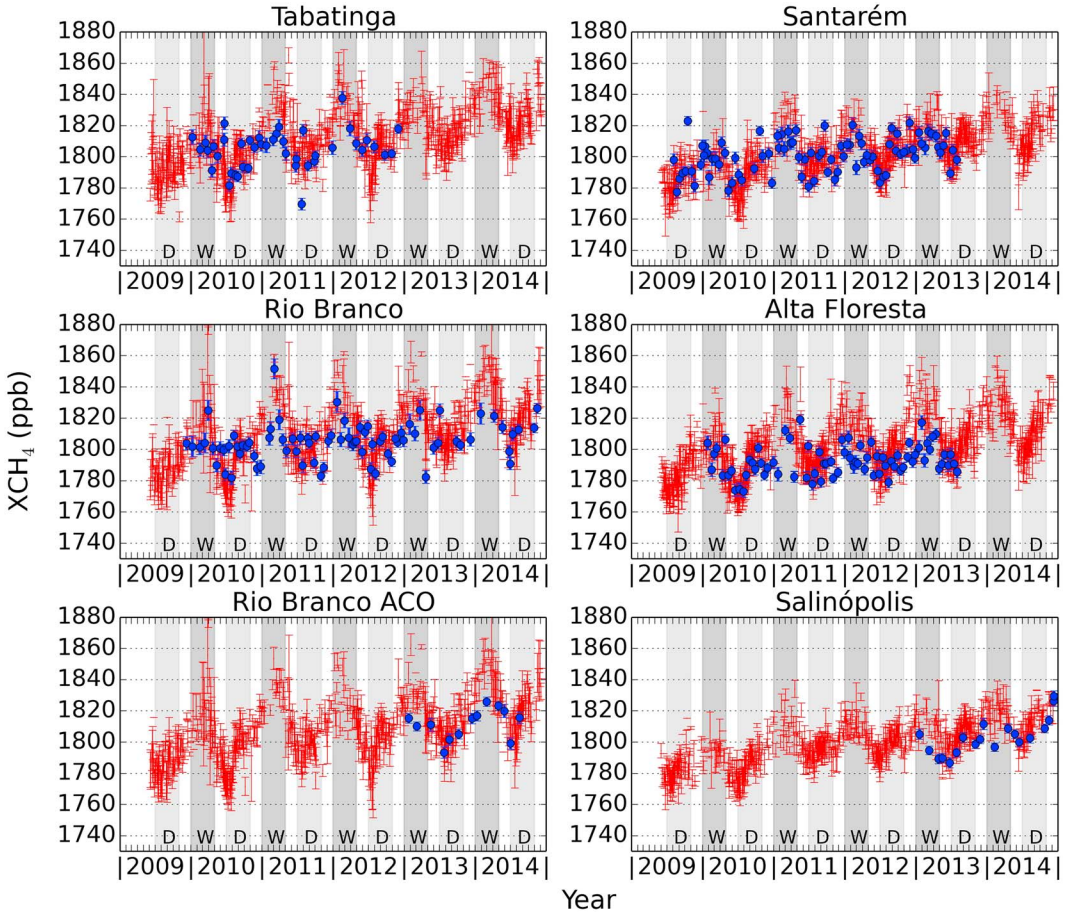

Figure 6. Methane concentration in parts per billion against the date of measurements for daily averaged GOSAT XCH_4 in red (error bars representing the standard error) and extended aircraft XCH_4 in blue. The approximate dry seasons (July–October) and wet seasons (January–April) are marked with D and W, respectively.

offsets without considering the weighting of the different flights (which are used for the offset and Pearson's *r* value calculations) indicates that the offsets observed are not significantly different from zero for TAB, SAN, RBA, and RBH, while at ALF and SAH the offsets are significant on a 95% but not a 98% level. The correlation coefficients (Pearson's *r*) are all above 0.6, showing that there is a reasonable to good agreement between aircraft and GOSAT XCH_4 at all of the sites. They are 0.74, 0.66, 0.61, and 0.68 for RBA, SAN, ALF, and TAB, respectively, and 0.90 and 0.61 for ACO sites RBH and SAH (using a ±5° colocation).

Of the AMAZONICA sites for which there are far more flights, the largest offset in XCH_4 is at Alta Floresta. This site also shows the largest variation in both the correlation coefficient and the offset over different colocation criteria (see Table 1). Furthermore, the largest difference in the XCO_2 between the offsets for different colocation criteria are also at ALF (as discussed in section 7). This could be due to the location of the site which is at the edge of the tropical Amazon, closer to the Cerrado ecosystem than the other aircraft sites. Fires are more prevalent in this region, and so ALF is likely more influenced by fires during the fire season than the other sites [*Gloor et al.*, 2012]. Previous studies [*Ross et al.*, 2013; *Parker et al.*, 2016] have shown that GOSAT measurements do show significantly changed total column CH_4 mole fractions in the presence of wildfires.

To assess the impact of the colocation criteria on the sampling of GOSAT XCH_4, we considered the use of different criteria (±5°, ±4°, ±3°, and ±2°, as shown in Table 1). The inferred offset values at RBA, RBH, and TAB each agree to within their uncertainties across all colocation criteria, while at SAN they do between ±5° and ±3°, and ALF and SAH between ±5° and ±4°. However, at ±2° around SAN and ±3° around ALF the number of flights which have matching GOSAT soundings decreases to only 13 and 9, respectively, compared to 46 and 32 at ±5°, which do not allow us to calculate a robust correlation coefficient with these small sample sizes. At SAH there are also only nine flights with coincident GOSAT at ±3°, but we lose more than half of

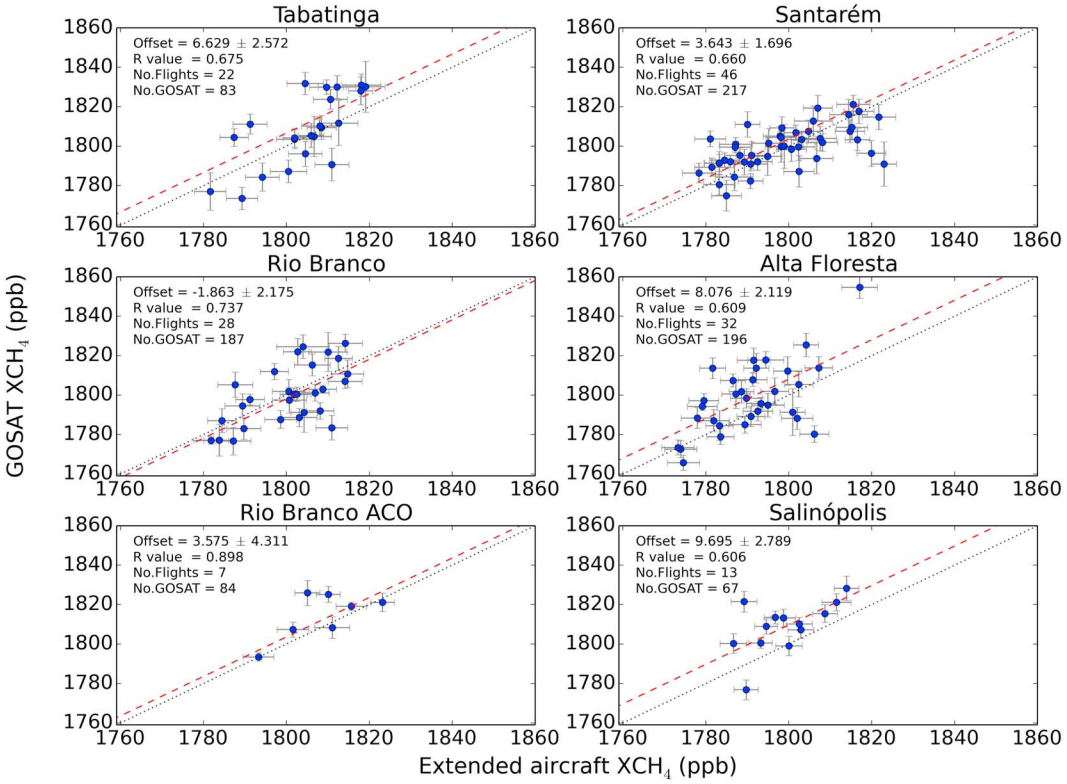

Figure 7. Correlation plot to illustrate the data shown in Table 1 for the case when the colocation criteria is ±5°. Showing the GOSAT XCH_4 on the *y* axis versus the aircraft XCH_4 on the *x* axis for the four AMAZONICA sites and two ACO sites. The black dotted line shows the one-to-one correlation line. The red dashed line shows the result of a linear regression with the slope set to one. From this the offset values given in Table 1 are the difference in intercept of each line with the *y* axis, giving the mean offset between GOSAT and aircraft XCH_4.

the GOSAT soundings compared to at ±5°. When using a stricter coincidence criterion, the coefficient of correlation remains consistent to within 0.14 except at ALF where the difference is larger (0.25) but remains a small difference. The correlation and bias between GOSAT and aircraft remain consistent with progressively smaller colocation criteria until the case where there are too few matches. Therefore, we chose to use the ±5° colocation criteria.

7. Assessing the Model XCO_2 Built Into the GOSAT Retrieval

To understand whether the model XCO_2, used in the proxy XCH_4 calculation, introduces biases in the GOSAT XCH_4 data, we compare the model XCO_2 to columns of XCO_2 calculated from the aircraft data by following the same method as detailed previously for XCH_4. For the stratosphere we have used the MACC-II v13r CO_2 model which utilizes surface flux observation networks. For the extrapolated region error analysis we use a high-resolution run which is driven by ERA-Interim operational high-resolution ECMWF meteorology. The results of this study are shown in Table 2 and show that there is only a small difference between the aircraft and model XCO_2. This difference is less than 0.58 ppm for every site and colocation criteria except for Rio Branco. Here the difference ranges from between 0.92 and 1.13 ppm. This difference in the model XCO_2 of 0.58 ppm to 1.13 ppm leads to differences in methane of approximately 2.6 ppb to 5.09 ppb, respectively, which are within GOSAT XCH_4 uncertainties. At ±5° colocation criteria the difference is particularly small at SAN, ALF, and TAB, relating to XCH_4 differences of less than 1 ppb at these sites (as small as 0.3 ppb at ALF) with uncertainties between 0.9 and 1.7 ppb. The correlation coefficients between the model and aircraft XCO_2 are high at all of the AMAZONICA sites and are above 0.9 at Alta Floresta, Rio Branco, and Santarém for all colocation criteria (0.93, 0.97, 0.90, and 0.76 for RBA, SAN, ALF, and TAB, respectively, for ±5°). The correlation coefficients are low at the ACO sites where we have only compared with flights in 2013 since the high-resolution model data were not available for 2014 (five flights with GOSAT matches for RBH ±5° and eight for SAH). The good correlation coefficients and small biases between the model XCO_2 used in the proxy retrieval and XCO_2 from aircraft

Table 1. Correlation Results With Varying Degrees of Filtering for the Extended Aircraft Profile XCH_4 Versus Same Day Averaged GOSAT XCH_4[a]

	Degrees			
Colocation Criteria	±5	±4	±3	±2
	Rio Branco (RBA)			
No. flights	28	18	11	9
No. GOSAT	187	128	67	33
R value	0.74	0.75	0.79	0.78
Offset (ppb)	−1.86	−1.42	−2.92	3.44
Offset error	2.18	2.69	3.56	3.83
	Santarém (SAN)			
No. flights	46	33	20	13
No. GOSAT	217	136	68	39
R value	0.66	0.66	0.70	0.74
Offset	3.64	4.08	4.12	8.46
Offset error	1.63	1.99	2.52	3.04
	Alta Floresta (ALF)			
No. flights	32	28	9	9
No. GOSAT	196	116	50	50
R value	0.61	0.37	0.63	0.63
Offset	8.08	10.14	15.64	15.64
Offset error	2.12	2.34	3.53	3.53
	Tabatinga (TAB)			
No. flights	22	14		
No. GOSAT	83	39		
R value	0.68	0.68		
Offset	6.63	8.51		
Offset error	2.57	3.21		
	Rio Branco ACO (RBH)			
No. flights	7	7	5	
No. GOSAT	84	77	52	
R value	0.90	0.89	0.96	
Offset	3.58	4.92	3.20	
Offset error	4.31	4.31	5.35	
	Salinópolis (SAH)			
No. flights	13	13	9	
No. GOSAT	67	52	27	
R value	0.61	0.65	0.50	
Offset	9.70	10.15	16.60	
Offset error	2.79	2.84	3.60	

[a]Only criteria with at least 10 coincident GOSAT retrievals are shown. Offset is calculated as described in text.

suggest that the XCO_2 model is unlikely to be causing the significant bias we observe at ALF in the proxy XCH_4; however, it could be contributing toward part of the biases at other sites. At Rio Branco this comparison suggests that the model XCO_2 could be low by approximately 0.92 ppm (for ±5° colocation criteria), which is equivalent to approximately 4.1 ppb in XCH_4. This difference may explain why GOSAT XCH_4 values at RBA are the lowest compared to aircraft of all of the sites (see Table 1).

Results of the aircraft campaigns are supported by comparisons between XCH_4 from GOSAT and the Paramaribo-FTS, shown in Figure 8. Between mid-2009 and 2013 there were five measurement campaigns,

Table 2. Correlation Results With Varying Degrees of Filtering for Extended Aircraft Profile XCO_2 Versus Same Day Averaged Model XCO_2 Which is Used in the University of Leicester Proxy Methane Retrieval (GEOS-Chem in This Study)[a]

	Degrees			
Colocation Criteria	±5	±4	±3	±2
	Rio Branco (RBA)			
Offset (ppm)	−0.92	−0.95	−1.02	−1.13
Offset error	0.42	0.55	0.60	0.52
R value	0.93	0.93	0.95	0.94
	Santarém (SAN)			
Offset	−0.22	−0.24	−0.25	−0.49
Offset error	0.19	0.23	0.29	0.32
R value	0.97	0.97	0.98	0.99
	Alta Floresta (ALF)			
Offset	−0.06	0.03	0.58	0.58
Offset error	0.38	0.41	0.84	0.84
R value	0.90	0.90	0.92	0.92
	Tabatinga (TAB)			
Offset	−0.22	−0.02		
Offset error	0.35	0.40		
R value	0.76	0.74		
	Rio Branco ACO (RBH)			
Offset	−0.44	−0.44	−0.19	
Offset error	0.65	0.66	0.90	
R value	0.33	0.33	0.96	
	Salinópolis (SAH)			
Offset	0.54	0.52	0.51	
Offset error	0.38	0.38	0.37	
R value	0.46	0.49	0.72	

[a]The aircraft profile XCO_2 is calculated in the same way as for the XCH_4 but instead using an ECMWF MACC CO_2 model for the stratosphere and a high-resolution version for the extrapolated region error analysis. The offset is calculated as the intercept on the Model XCO_2 axis when a linear function of gradient 1 is fit to the data.

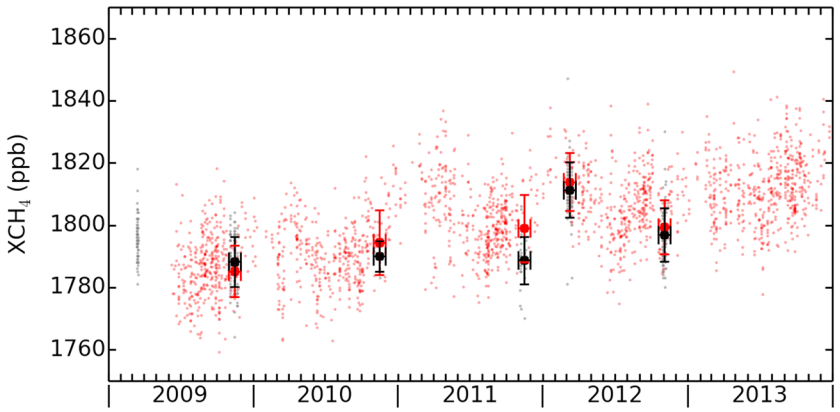

Figure 8. Showing comparisons between Paramaribo-FTS (black) and GOSAT (red) for XCH_4. The lighter shaded scatter points show all of the Paramaribo-FTS data between 2009 and 2013 and all GOSAT until the end of 2013 which is within ±5° of the site. The average of Paramaribo-FTS data (standard deviation given in *y* direction error bars) for each campaign period (shown in *x* direction error bars) and coincident GOSAT within the same time period is averaged and also plotted.

providing 306 ground-based XCH_4 measurements with, in total, 109 coincident GOSAT soundings within ±1 day and ±5° of these measurements. In Figure 8 we show these measurements in context with the spatially coincident GOSAT soundings for the entire time period, and to highlight the campaign periods further, we plot the averages over these time periods (with the *x* axis error bars indicating the time period and the *y* axis error bars indicating the standard deviation of the encompassed XCH_4 data). The XCH_4 measured at the FTS site agrees well with the GOSAT data ($r = 0.89$), and GOSAT tends to be higher by 3.4 ± 2.1 ppb across all campaigns (although the uncertainties do overlap for each of these periods).

8. Summary and Conclusion

The tropics are an important region for CH_4 fluxes to the atmosphere; however, tropical greenhouse gas concentrations are strongly undersampled. Satellites such as GOSAT can potentially provide much needed observations here, but their current usefulness is limited due to their lack of validation in the tropics. Recently, vertical profile data measured in situ over the Amazon have become available, and we present new measurements from 300 m asl up to 7.5 km altitude taken between 2013 and mid-2015 at two sites in the Amazon, chosen specifically to represent air before and after traveling across the Basin. These profiles show a distinct seasonality, with the inland site exhibiting enhanced CH_4 concentrations in the wet season compared to those at the coastal site. Here we use these data for the first time to validate GOSAT remote sensing XCH_4 retrievals over the Amazon and determine whether or not they agree with in situ vertical CH_4 profiles sampled at these two sites in the Amazon. Additional profiles extending from 300 m asl up to 4.5 km altitude measured during the AMAZONICA project have also been used at four sites. The aircraft profiles, which reach up to 4.5 km and 7.5 km, were extended using a stratospheric chemistry model and by extrapolating throughout the remainder of the troposphere. The random and systematic uncertainties involved in this method were estimated by examining the variation of methane in a high-resolution model, and the difference between the 4.5 km and 7.5 km heights was evaluated. This shows a possible systematic bias in our method; however, it is shown that in the majority of cases the magnitude of this error combined with the random uncertainty is still smaller than the uncertainty of coincident GOSAT soundings. The average systematic uncertainty across all flights year round at each site accounts for 1.65 ppb for AMAZONICA sites and 1.13 ppb for ACO sites, with maximum uncertainties of 5 ppb. The analysis into the effect of using our 7.5 km aircraft profiles compared to 4.5 km profiles shows that both the random and systematic uncertainties can be significantly reduced by measuring to higher altitudes. Choosing a coarse colocation criteria can introduce colocation errors, but a very strict criterion leads to a small sample set (and thus to poor statistics) due to the sparseness of GOSAT soundings. We find that using a ±5° colocation criteria is preferable over smaller colocation criteria. Overall, this study highlights the importance of aircraft and ground-based measurements to diagnose potential biases in satellite data which inverse methods are sensitive to.

We find good agreement between in situ data extrapolated throughout the atmosphere and the remote sensing data from GOSAT in respect to the seasonality of XCH_4 measurements. The absolute concentrations agree within uncertainties or show no significant difference (Student's *t* test) at three of the aircraft sites (−1.9 ± 2.2 ppb for RBA, 3.6 ± 4.3 ppb for RBH, 3.6 ± 1.7 ppb for SAN, and 6.6 ± 2.6 ppb for TAB), while the other two show GOSAT to be slightly higher than aircraft measurements, by up to approximately 10 ppb in the most differing case (8.1 ± 2.1 ppb for ALF and 9.7 ± 2.8 ppb for SAH). These results are consistent with results by *Inoue et al.* [2014, 2016] who compare GOSAT with aircraft measurements at 17 stations (outside of the Amazon) and find that over land with the same ±5° colocation we use, GOSAT showed a positive station bias of 3.4 ± 7.0 ppb. Uncertainties introduced by the model XCO_2 in the proxy XCH_4 method could account for part of the biases we observe, especially at RBA where the model is shown to be the lowest compared to aircraft measurements. This may explain why XCH_4 at RBA is also low compared to aircraft data. While these potential biases of 10 ppb are small compared to the regional fluxes we observe (on the order of 50 ppb), they are still significant. However, it is difficult to know how they would bias estimated surface fluxes without more analysis into how such biases map into fluxes. Measurements from a ground-based FTS at Paramaribo have also been compared with GOSAT and are found to be in agreement within their uncertainties. Satellite-retrieved XCH_4 fields over tropical South America tend to show elevated levels in the northwest corner of the continent in the dry seasons, while in the wet seasons GOSAT observes enhanced concentrations throughout much of the Amazon Basin. The largest enhancements are seen to coincide with a region known to contain vast wetlands. The fairly small difference between the extrapolated in situ observations and the GOSAT remote sensing data is encouraging evidence that remotely sensed atmospheric XCH_4 data from GOSAT have a small bias over the

Amazon and can provide new insights into wetland CH_4 emissions in the Amazon. This better understanding of bias in GOSAT XCH_4 measurements can therefore provide us with improved top-down surface flux estimates of CH_4 in the Amazon, which could help to resolve some of the discrepancies between models, as were highlighted by *Melton et al.* [2013].

Acknowledgments
We thank JAXA and NIES for providing access and support for GOSAT data. We thank the NERC and FAPESP for their joint funding of the Amazonian Carbon Observatory Project (NERC Reference: NE/J016284/1). A. Webb is funded by the UK Natural Environment Research Council (NERC). H. Bösch and R. Parker are supported by the NERC National Centre for Earth Observation (NCEO) and the ESA Climate Change Initiative (GHG-CCI). Parker is also funded via an ESA Living Planet Fellowship. M. Gloor was financially supported by the NERC consortium grant AMAZONICA (NE/F005806/1) which we also thank for providing access to additional aircraft profiles. We thank BADC for providing ECMWF data. Research at the University of Edinburgh is funded by the NERC grant NE/J016195/1. P. Palmer acknowledges his Royal Society Wolfson Research Merit Award. The University of Leicester GOSAT data are freely available through the ESA GHG-CCI website (www.esa-ghg-cci.org). ACO data will be made available through the British Atmospheric Data Centre (BADC) (www.badc.nerc.ac.uk/data/), and AMAZONICA data are available upon request by L. V. Gatti (lvgatti@gmail.com). ECMWF ERA-Interim data are available through the ECMWF website (http://apps.ecmwf.int/datasets/). Access to the MACC-II data can be requested from the ECMWF MARS data server (experiment ID g4om, www.ecmwf.int/en/forecasts/datasets). Paramaribo-FTS data are available upon request from T. Warneke (warneke@iup.physik.uni-bremen.de). GEOS-Chem model and metadata are freely available upon request by P. Palmer (pip@ed.ac.uk). TOMCAT model output can be requested from M. Chipperfield (M.Chipperfield@leeds.ac.uk), who acknowledges his Royal Society Wolfson Research Merit award. This research used the SPECTRE and ALICE High Performance Computing Facilities at the University of Leicester. The TOMCAT model was run on the Archer national supercomputer. We thank CEDA for use of the JASMIN supercomputer system on which we run the NAME model.

References

Alexe, M., et al. (2015), Inverse modelling of CH_4 emissions for 2010–2011 using different satellite retrieval products from GOSAT and SCIAMACHY, *Atmos. Chem. Phys.*, *15*, 113–133, doi:10.5194/acp-15-113-2015.

Bergamaschi, P., et al. (2009), Inverse modeling of global and regional CH4 emissions using SCIAMACHY satellite retrievals, *J. Geophys. Res.*, *114*, D22301, doi:10.1029/2009JD012287.

Bloom, A. A., P. I. Palmer, A. Fraser, and D. S. Reay (2012), Seasonal variability of tropical wetland CH_4 emissions: The role of the methanogen-available carbon pool, *Biogeosciences*, *9*, 2821–2830, doi:10.5194/bg-9-2821-2012.

Chipperfield, M. P. (1999), Multiannual simulations with a three-dimensional chemical transport model, *J. Geophys. Res.*, *104*, 1781–1805, doi:10.1029/98JD02597.

Ciais, P., et al. (2013), Carbon and other biogeochemical cycles, in *Climate Change 2013: The Physical Science Basis. Contribution of Working Group I to the Fifth Assessment Report of the Intergovernmental Panel on Climate Change*, edited by T. F. Stocker et al., pp. 473–507, Cambridge Univ. Press, Cambridge, U. K. and New York.

De Mazière, M., et al. (2008), Validation of ACE-FTS v2.2 methane profiles from the upper troposphere to the lower mesosphere, *Atmos. Chem. Phys.*, *8*, 2421–2435, doi:10.5194/acp-8-2421-2008.

Dils, B., et al. (2014), The Greenhouse Gas Climate Change Initiative (GHG-CCI): Comparative validation of GHG-CCI SCIAMACHY/ENVISAT and TANSO-FTS/GOSAT CO_2 and CH_4 retrieval algorithm products with measurements from the TCCON, *Atmos. Meas. Tech.*, *7*(6), 1723–1744, doi:10.5194/amt-7-1723-2014.

Dlugokencky, E. J., L. P. Steele, P. M. Lang, and K. A. Masarie (1994), The growth rate and distribution of atmospheric methane, *J. Geophys. Res.*, *99*(D8), 17021–17043, doi:10.1029/94JD01245.

Dlugokencky, E. J., S. Houweling, L Bruhwiler, K. A. Masarie, P. M. Lang, J. B. Miller, and P. P. Tans (2003), Atmospheric methane levels off: Temporary pause or a new steady-state, *Geophys. Res. Lett.*, *30*(19), 1992, doi:10.1029/2003GL018126.

Draxler, R. R., and G. D. Hess (1997), Description of the HYSPLIT4 modeling system, *NOAA Tech. Memo. ERL ARL-224*, 24 pp., NOAA Air Resources Laboratory, Silver Spring, Md.

Feng, L., P. I. Palmer, H. Bösch, and S. Dance (2009), Estimating surface CO_2 fluxes from space-borne CO_2 dry air mole fraction observations using an ensemble Kalman filter, *Atmos. Chem. Phys.*, *9*, 2619–2633, doi:10.5194/acp-9-2619-2009.

Feng, L., P. I. Palmer, Y., Yang, R. M. Yantosca, S. R. Kawa, J.-D. Paris, H. Matsueda, and T. Machida (2011), Evaluating a 3-D transport model of atmospheric CO_2 using ground-based, aircraft, and space-borne data, *Atmos. Chem. Phys.*, *11*, 2789–2803, doi:10.5194/acp-11-2789-2011.

Frankenberg, C., J. F. Meirink, P. Bergamaschi, A. P. H. Goede, M. Heimann, S. Körner, U. Platt, M. van Weele, and T. Wagner (2006), Satellite chartography of atmospheric methane from SCIAMACHY on board ENVISAT: Analysis of the years 2003 and 2004, *J. Geophys. Res.*, *111*, D07303, doi:10.1029/2005JD006235.

Fraser, A., et al. (2013), Estimating regional methane surface fluxes: The relative importance of surface and GOSAT mole fraction measurements, *Atmos. Chem. Phys.*, *13*, 5697–5713, doi:10.5194/acp-13-5697-2013.

Fraser, A., P. I. Palmer, L. Feng, H. Boesch, R. Parker, E. J. Dlugokencky, P. B. Krummel, and R. L. Langenfelds (2014), Estimating regional fluxes of CO_2 and CH_4 using space-borne observations of XCH4:XCO2, *Atmos. Chem. Phys*, *14*, doi:10.5194/acp-14-12883-2014.

Gatti, L. V., et al. (2014), Drought sensitivity of Amazonian carbon balance revealed by atmospheric measurements, *Nature*, *506*(7486), 76–80, doi:10.1038/nature12957.

Gloor, M., et al. (2012), The carbon balance of South America: A review of the status, decadal trends and main determinants, *Biogeosciences*, *9*, 5407–5430, doi:10.5194/bg-9-5407-2012.

Hess, L. L., J. M. Melack, A. G. Affonso, C. Barbosa, M. Gastil-Buhl, and E. M. L. M. Novo (2015), Wetlands of the lowland Amazon Basin: Extent, vegetative cover, and dual-season inundated area as mapped with JERS-1 synthetic aperture radar, *Wetlands*, *35*, 754–756, doi:10.1007/s13157-015-0666-y.

Inoue, M., et al. (2014), Validation of XCH_4 derived from SWIR spectra of GOSAT TANSO-FTS with aircraft measurement data, *Atmos. Meas. Tech.*, *7*, 2987–3005, doi:10.5194/amt-7-2987-2014.

Inoue, M., et al. (2016), Bias corrections of GOSAT SWIR XCO_2 and XCH_4 with TCCON data and their evaluation using aircraft measurement data, *Atmos. Meas. Tech.*, *9*, 3491–3512, doi:10.5194/amt-9-3491-2016.

Jones, A. R., D. J. Thomson, M. Hort, and B. Devenish (2007), The U. K. Met Office's next-generation atmospheric dispersion model, NAME III, in *Proceedings of the 27th NATO/CCMS International Technical Meeting on Air Pollution Modelling and its Application, Air Pollution Modeling and its Application XVII*, edited by C. Borrego and A.-L. Norman, pp. 580–589, Springer, U.S.A., doi:10.1007/978-0-387-68854-1-62.

Kalney, E., et al. (1996), The NCEP/NCAR 40-year reanalysis project, *Bull. Amer. Meteor. Soc.*, *77*, 437–471, doi:10.1175/1520-0477(1996)077<0437:TNYRP>2.0.CO;2.

Kirschke, S., et al. (2013), Three decades of global methane sources and sinks, *Nat. Geosci.*, *6*, 813–823, doi:10.1038/ngeo1955.

Kuze, A., H. Suto, M. Nakajima, and T. Hamazaki (2009), Thermal and near infrared sensor for carbon observation Fourier-transform spectrometer on the Greenhouse Gases Observing Satellite for greenhouse gases monitoring, *Appl. Opt.*, *48*(35), 6716–6733, doi:10.1364/AO.48.006716.

Kuze, A., et al. (2016), Update on GOSAT TANSO-FTS performance, operations, and data products after more than six years in space, *Atmos. Meas. Tech. Disscuss.*, 1–38, doi:10.5194/amt-2015-333.

Melton, J. R., et al. (2013), Present state of global wetland extent and wetland methane modelling: Conclusions from a model inter-comparison project (WETCHIMP), *Biogeosciences*, *10*, 753–788, doi:10.5194/bg-10-753-2013.

Miller, J. B., L. V. Gatti, M. T. S. d'Amelio, A. M. Crotwell, E. J. Dlugokencky, P. Bakwin, P. Artaxo, and P. P. Tans (2007), Airborne measurements indicate large methane emissions from the eastern Amazon Basin, *Geophys. Res. Lett.*, *34*, L10809, doi:10.1029/2006GL029213.

Miyamoto, Y., et al. (2013), Atmospheric column-averaged mole fractions of carbon dioxide at 53 aircraft measurement sites, *Atmos. Chem. Phys.*, *13*(10), 5265–5275, doi:10.5194/acp-13-5265-2013.

Nisbet, E. G., E. J. Dlugokencky, and P. Bousquet (2014), Methane on the rise-again, *Science*, *343*(6170), 493–495, doi:10.1126/science.1247828.

O'Dell, C. W., et al. (2012), The ACOS CO_2 retrieval algorithm—Part 1: Description and validation against synthetic observations, *Atmos. Meas. Tech.*, *5*(1), 99–121, doi:10.5194/amt-5-99-2012.

Pandey, S., S. Houweling, M. Krol, I. Aben, and T Röckmann (2015), On the use of satellite-derived CH_4:CO_2 columns in a joint inversion of CH_4 and CO_2 fluxes, *Atmos. Chem. Phys.*, *15*, 8615–8629, doi:10.5194/acp-15-8615-2015.

Pandey, S., et al. (2016), Inverse modeling of GOSAT-retrieved ratios of total column CH_4 and CO_2 for 2009 and 2010, *Atmos. Chem. Phys.*, *16*, 5043–5062, doi:10.5194/acp-16-5043-2016.

Parker, R., H. Boesch, A. Cogan, A. Fraser, L. Feng, P. I. Palmer, and D. Wunch (2011), Methane observations from the Greenhouse Gases Observing SATellite: Comparison to ground-based TCCON data and model calculations, *Geophys. Res. Lett.*, *38*, L15807, doi:10.1029/2011GL047871.

Parker, R., et al. (2015), Assessing 5 years of GOSAT Proxy XCH_4 data and associated uncertainties, *Atmos. Meas. Tech.*, *8*, 4785–4801, doi:10.5194/amt-8-4785-2015.

Parker, R. J., H. Boesch, M. J. Wooster, D. P. Moore, A. J. Webb, D. Gaveau, and D. Murdiyarso (2016), Atmospheric CH_4 and CO_2 enhancements and biomass burning emission ratios derived from satellite observations of the 2015 Indonesian fire plumes, *Atmos. Chem. Phys.*, *16*(15), 10111–10131, doi:10.5194/acp-16-10111-2016.

Prather, M. (1986), Numberical advection by conservation of second-order moments, *J. Geophys. Res. Atmos.*, *91*, 6671–6681, doi:10.1029/JD091iD06p06671.

Reichler, T., M. Dameris, and R. Sausen (2003), Determining the tropopause height from gridded data, *Geophys. Res. Lett.*, *30*(20), 2042, doi:10.1029/2003GL018240.

Rigby, M., et al. (2008), Renewed growth of atmospheric methane, *Geophys. Res. Lett.*, *35*, L22805, doi:10.1029/2008GL036037.

Ross, A. N., M. J. Wooster, H. Boesch, and R. Parker (2013), First satellite measurements of carbon dioxide and methane emission ratios in wildfire plumes, *Geophys. Res. Lett.*, *40*, 4098–4102, doi:10.1002/grl.50733.

Schepers, D., et al. (2012), Methane retrievals from Greenhouse Gases Observing Satellite (GOSAT) shortwave infrared measurements: Performance comparison of proxy and physics retrieval algorithms, *J. Geophys. Res.*, *117*, D10307, doi:10.1029/2012JD017549.

Warneke, T., A. K. Petersen, C. Gerbig, A. Jordan, C. Rödenbeck, M. Rothe, R. Macatangay, J. Notholt, and O. Schrems (2010), Co-located column and in situ measurements of CO_2 in the tropics compared with model simulations, *Atmos. Chem. Phys.*, *10*, 5593–5599, doi:10.5194/acp-10-5593-2010.

Wilson, C., M. Gloor, L. V. Gatti, J. B. Miller, S. A. Monks, J. McNorton, A. A. Bloom, L. S. Basso, and M. P. Chipperfield (2015), Contribution of regional sources to atmospheric methane over the Amazon Basin in 2010 and 2011, *Global Biogeochem. Cycles*, *30*(3), 400–420, doi:10.1002/2015GB005300.

Wunch, D., et al. (2010), Calibration of the total carbon column observing network using aircraft profile data, *Atmos. Meas. Tech.*, *3*(5), 1351–1362, doi:10.5194/amt-3-1351-2010.

Wunch, D., G. C. Toon, J-F. L. Blavier, R. A. Washenfelder, J. Notholt, B. J. Connor, D. W. T. Griffith, V. Sherlock, and P. O. Wennberg (2011), The total carbon column observing network, *Philos. Trans. R. Soc. A*, *369*(1943), 2087–2112, doi:10.1098/rsta.2010.0240.

Yokota, T., Y. Yoshida, N. Eguchi, Y. Ota, T. Tanaka, H. Watanabe, and S. Maksyutov (2009), Global concentrations of CO_2 and CH_4 retrieved from GOSAT: First preliminary results, *Sci. Online Lett. Atmos.*, *5*, 160–163, doi:10.2151/sola.2009-041.